Available online at www.sciencedirect.com
SCIENCE DIRECT
Polymer 46 (2005) 12703–12710
polymer
www.elsevier.com/locate/polymer

Synthesis and stimuli-responsive properties of chitosan/poly(acrylic acid) hollow nanospheres

Yong Hu [a], Ying Chen [a], Qi Chen [a], Leyang Zhang [a], Xiqun Jiang [a,b,*], Changzheng Yang [a]

[a] *Laboratory of Mesoscopic Chemistry and Department of Polymer Science and Engineering, College of Chemistry and Chemical Engineering, Nanjing University, Nanjing 210093, China*
[b] *Jiangsu Provincial Laboratory for Nanotechnology, Nanjing University, Nanjing, China*

Received 25 May 2005; received in revised form 4 October 2005; accepted 25 October 2005
Available online 11 November 2005

Abstract

We report here a synthetic study on the formation process of hollow polymeric nanospheres based on a simple, core-template-free route, and the effects of polymerization concentration, shell cross-linking, pH, salt concentration and temperature on the size and stability of hollow polymeric nanospheres. The hollow structure of polymeric nanospheres is spontaneously formed by polymerization of acrylic acid monomers inside the chitosan–acrylic acid assemblies. It is found that (i) the hollow structure of nanospheres is stabilized by both physical cross-linking in the inner shell and chemical cross-linking in the outmost shell; (ii) the size of the hollow spheres can be adjusted over the range of 77–500 nm by controlling the concentration of chitosan–acrylic acid assemblies in the reaction system; (iii) the synthesized nanospheres are stimuli-responsive. The size of the hollow nanospheres can be manipulated by changing pH, salt concentration and temperature. Furthermore, with heating and cooling the variation in size of hollow nanospheres is completely reversible and reproducible; (iv) the surface of the hollow nanospheres obtained is chemically active, which provides the functional sites with chemical groups for subsequent chemical reactions at the surface.

Keywords: Chitosan; Poly(acrylic acid); Hollow nanospheres

1. Introduction

The design and synthesis of nanosized polymer materials are the focus of intensive investigations because such materials can be widely used in optics [1], electronics [2], and biotechnology [3,4]. In biotechnology and medicine, by controlling the composition, structure, and function of the nanosized polymer materials, such as nanoparticles [5], nanocapsules [6], and micelles [7], they can serve as the effective vehicles for drug delivery, drug controlled release and gene therapy. Among these nanosized polymer materials, hollow polymeric nanospheres obtained particular interest because of their great potential ability to encapsulate large quantities of therapeutic and diagnostic agents in their hollow inner cavities and release them at later stage. Such encapsulation can greatly increase drug bioavailability, protect agents from destructive factors upon parenteral administration, and modify their pharmacokinetics and biodistribution in body [8]. In addition, as DNA carriers, they can be taken up by cells via receptor-mediated endocytosis pathway if their size is less than 150 nm [9].

Various methods, such as the self-assembly of block copolymers in selective solvent [10,11], layer-by-layer deposition of polyelectrolytes on sacrificial core [12,13], and microemulsion as well as miniemulsion polymerization [14,15], have been developed to fabricate hollow polymeric spheres. However, these methods require multiple steps and severe synthesis conditions, and need the removal of the sacrificial core to create a hollow structure. Furthermore, the size of spheres is limited by block length of block copolymers and the templates used. On the other hand, although the majority of the proposed applications of hollow nanospheres or nanocapsules are concentrated on biomedical area, most of the hollow polymeric spheres described up to now are not well-suited. Therefore, in terms of practical applications of the hollow polymeric spheres in biomedical area, the preparation of polymeric hollow spheres with a larger-scale in quantities by a simple method using biocompatible and biodegradable

* Corresponding author. Address: Laboratory of Mesoscopic Chemistry and Department of Polymer Science and Engineering, College of Chemistry and Chemical Engineering, Nanjing University, Nanjing 210093, China. Fax: +86 25 3317761.
E-mail address: jiangx@nju.edu.cn (X. Jiang).

0032-3861/$ - see front matter © 2005 Elsevier Ltd. All rights reserved.
doi:10.1016/j.polymer.2005.10.110

materials, and the capability of hollow spheres to respond to external stimuli such as temperature and pH, are highly desirable [16,17].

In previous works, we reported a simple core-template-free strategy to prepare hollow polymeric nanospheres and hollow composite nanospheres in complete aqueous solution using chitosan (CS) and acrylic acid (AA) as a reaction system [18,19]. We found that CS could interact with AA and such interaction induced amphiphilicity and resulted in spontaneous assembly between CS and AA in reaction system. When AA monomers were polymerized in complete aqueous solution, the hollow polymeric nanospheres are spontaneously formed. However, the formation mechanism and the size control as well as the stimuli-responsive properties of chitosan-poly(acrylic acid) (CS–PAA) hollow nanospheres are unprecedented. In this article, we provide the results studying on the formation process and mechanism of CS–PAA hollow nanospheres, and the effects of polymerization concentration, shell cross-linking, pH, salt concentration and temperatures on the size and stability of hollow polymeric nanospheres.

2. Experimental section

2.1. Materials

Chitosan (CS) (Nantong Shuanglin Biological Product Inc.) was refined twice by being dissolved in dilute acetic acid solution, filtered, precipitated with aqueous NaOH, and finally dried in a vacuum at room temperature. The degree of deacetylation was about 88%, and average molecular weight of chitosan was 200 kDa, determined by viscometric method [20]. Potassium persulfate ($K_2S_2O_8$) was recrystallized from distilled water. Acrylic acid (AA) (Shanghai Guanghua Chemical Company) was distilled under reduced pressure in nitrogen atmosphere. Glutaraldehyde (GA) was purchased from Sigama Chemical Company (St Louis, MO). All other reagents were of analytical grade and used without further purification.

2.2. Synthesis

Purified CS (0.5 g) was dissolved in 50 mL acrylic acid aqueous solution with 0.22 g acrylic acid. The concentration of CS and AA in reaction system was 14.4 g/L (except when otherwise stated) and the molar ratio of glucosamine unit in CS to acid in AA was 1.1:1. Until the solution became clear, the polymerization was initiated by $K_2S_2O_8$ at 80 °C under a nitrogen stream and magnetic stirring. As the reaction mixture appeared opalescent, the reaction was allowed to proceed for another 60–100 min at 60 °C. The sample was then filtered to remove polymer aggregates. The residual monomers were removed by dialysis in a buffer solution of pH = 4.5 for 24 h using a dialysis membrane bag (12 kDa cut off). After this, a determined amount of glutaraldehyde, in the ratio of glucosamine unit in CS to aldehyde unit in GA of 2 (except when otherwise stated), was added to this system and continued to react for 2 h at 40 °C.

2.3. Dynamic light scattering

Hydrodynamic diameter and size distribution of the prepared hollow nanospheres were determined by dynamic light scattering (DLS) method using a Brookhaven BI9000AT system (Brookheaven Instruments Corporation, USA). All the measurements were repeated 3 times with a wavelength of 658.0 nm. Before measurement, samples were diluted to proper concentration.

2.4. Zeta potential analysis

Zeta potential of the hollow nanospheres was obtained with Zetaplus (Brookhaven Instruments Corporation, USA). Each sample of the sphere suspension was adjusted to a concentration of 0.1% (wt/v) in 10 mmol/L NaCl solution. All analyses were triplicated and the results were the average of three runs.

2.5. Transmission electron microscopy

Transmission electron microscopy (TEM) observation was performed on a JEOL TEM-100, Japan. The samples were placed on nitrocellulose covered copper grid at room temperature. For microtomying samples, an aqueous suspension of the cross-linked nanospheres was frozen at −80 °C for 24 h, and then the sample was lyophilized to dry powder. A few granules of the resulting powder were embedded in epoxy resin and sections of about 70 nm thick were obtained by microtoming the resin sample at room temperature.

2.6. Atomic force microscopy

Atomic force microscopy (AFM) (SPI3800, Seiko Instruments Inc, Japan) was used to study the surface morphology of spheres in a greater detail. One drop of properly diluted sphere suspension was placed on the surface of a clean silicon wafer and dried under nitrogen flow at room temperature. The AFM observation was performed with a 20-micrometer scanner in tapping mode. The phase images were obtained by operating the instrument in the tapping mode under ambient conditions. The phase images represent the variations of relative phase shifts and are thus able to distinguish materials by their material properties.

3. Results and discussion

3.1. The preparation and morphology of CS–PAA nanospheres

The chitosan–poly(acrylic acid) (CS–PAA) hollow nanospheres used in present studies were synthesized by dissolving CS into AA aqueous solution with the concentration of 14.4 g/L (CS + AA) and the ratio of 1.1:1 ([glucosamine unit in CS]:[acid in AA]), followed by polymerization of AA

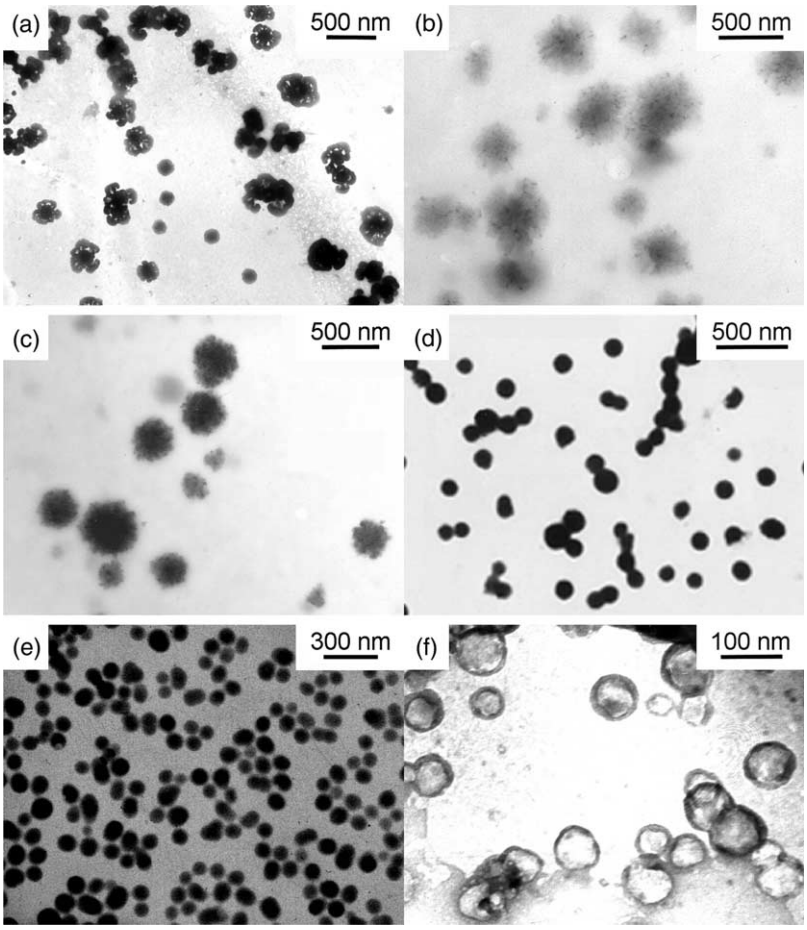

Fig. 1. Morphology of the assemblies at different polymerization time (t). (a) $t=0$; (b) $t=30$ min; (c) $t=50$ min; (d) $t=120$ min; (e) after chemically cross-linking of nanospheres in (d), and (f) cut-section TEM image of assemblies in (e) after microtoming.

initiated by $K_2S_2O_8$, and then selective cross-linking of CS at the end of polymerization using glutaraldehyde. First, we used TEM to observe the morphologies of the samples at different stages. Fig. 1 shows the TEM images of the samples at different polymerization times. It can be seen that the micelle-like structure with the size of 450 ± 50 nm was formed before the polymerization (Fig. 1(a)), suggesting that the assembly between CS and AA is achieved by the electrostatic interaction between protonated CS and dissociated AA. At this stage, the pH value in solution and ζ potential for the assemblies were measured to be 4.1 and 67.3 mV, respectively. The salient feature of the assemblies in this stage is their core-shell structure. This is different from the situation in which the spherical assemblies were formed by poly-L-lysine and certain small molecular multicarboxylic acids [21]. Based on the ionization degrees of CS and AA calculated at this stage [18] and the ζ potential measured, the swelling shells shown in Fig. 1(a) can be deduced to be positively charged protonated CS chains, while the cores are comprised mainly of the polyion complexes of CS and AA (i.e. positively charged protonated CS chains and negatively charged dissociated acrylic acid). Since the core is charge-neutral, it should be somewhat hydrophobic compared with the cationic shell. When the polymerization starts, the morphology of assemblies changes upon the polymerization of AA. At the polymerization time of 30 min, the assemblies tend to become spherical in shape (Fig. 1(b)), but a loose shell structure is still present and the assemblies appear smaller than those in the initial stage. When the polymerization time extends to 50 min, the morphology of assemblies becomes more spherical in shape and the swollen shell decreases markedly (Fig. 1(c)). At the end of the polymerization, CS–PAA nanospheres with a diameter about 118 ± 15 nm are formed and the swollen shell almost disappears (Fig. 1(d)). At this time, a positive ζ potential (25 mV) is still maintained. After selectively cross-linking the CS shell layer using GA for 2 h, the diameter of the assemblies further decreases to 85 ± 11 nm (Fig. 1(e)).

In order to study the internal morphology of chemically cross-linked CS–PAA assemblies, thin sections of about 70 nm were prepared by microtomy at room temperature of specimens embedded in epoxy resin. A TEM image of a section of the CS–PAA assemblies shows that the resulting assemblies are the nanospheres having a hollow structure in the interior after chemically cross-linking (Fig. 1(f)). Close examination of the sphere shells, one can see that the dark ring is present in the inner shell of these hollow nanospheres. We ascribe this ring to interpolyelectrolyte complex layer between CS and PAA. The presence of this layer in the inner shell of the hollow

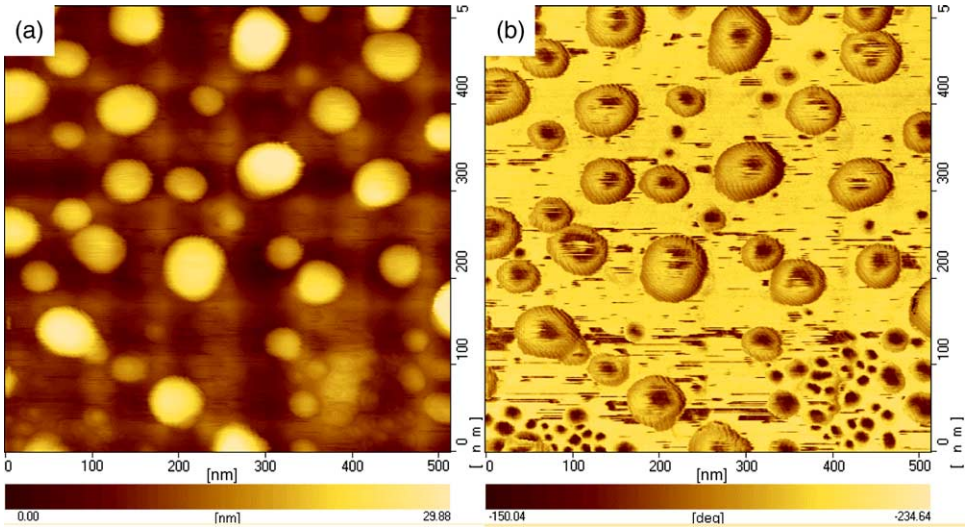

Fig. 2. AFM images of chemically cross-linked CS–PAA hollow nanospheres. (a) height image, and (b) phase image.

nanospheres indicates that the formation of hollow structure is induced by the polymerization of AA monomers inside core-shell assemblies. Thus, combining the cut-section TEM image and the positive ζ potential of nanospheres, it seems safe to conclude that hollow nanospheres are comprised of protonated CS chains as the outer shell and CS–PAA interpolyelectrolyte complexes (IPEC) as the inner shell. It should be noted that there are two kinds of the factors to maintain the hollow structure to be stable: one is physically cross-linking IPEC in the inner shell and another is chemically cross-linking in the outmost shell.

AFM imaging provides further evidence for the morphology of the obtained hollow nanospheres. As seen from height image in Fig. 2(a), the chemically cross-linked CS–PAA nanospheres appear as the intact spheres with an average width of 61 ± 11 nm and an average height of 25 ± 4 nm, while in phase image of Fig. 2(b), the bright spherical bodies with dark center are observed. The bright regions in phase image correspond to hard part and the dark regions correspond to soft part. Apparently, the center of nanospheres is very soft, which well corresponds to the hollow structure of nanospheres.

3.2. The formation mechanism of these CS–PAA nanospheres

We next used DLS to estimate the size and size distribution of samples in aqueous solution during the polymerization. Fig. 3 presents the size distribution obtained at different polymerization stages and after shell cross-linking. At the initial stage of polymerization, the size distribution of samples shows two peaks. As the polymerization is continued, both peaks shift progressively to the smaller intensity-average hydrodynamic diameter (D_h), and merge into a single peak after polymerization time reaches 120 min. Upon the shell cross-linking, the size of the spheres decreases further and the size distribution becomes narrow. Although the size of samples in aqueous solution is larger than that in dried state, the variation in size is in good agreement with the TEM observation.

A possible transition mechanism between micelle and hollow nanosphere can be considered as follows (Fig. 4). The key step in the synthesis of hollow nanosphere is that CS molecules can be dissolved into AA aqueous solution and bind electrostatically to the negatively charged dissociated acrylic acid to form core-shell assemblies. Since the ionization degree of CS molecules is larger than that of AA molecules at given pH value of 4.1 ($pKa = 6.0$ and 4.26 for CS and AA, respectively), the CS–AA assemblies are stabilized by the positively charged CS chains in the shells. Upon polymerization of AA, PAAs were generated and interacted with CS chains to form water-insoluble and hydrophobic IPEC. Progressively, such interaction enhanced with the polymerization progressing, which causes the assemblies from a loose core-shell structure to become gradually a dense spherical structure and leads to a decrease in the size of assemblies, as shown by TEM images and DLS measurements. This process experiences two kinds of force: an electrostatic attractive force between CS and PAA drawing spheres shrinkage, and an electrostatic repulsive force from the positively charged shell, which tends to expand the spheres. The equilibrium resultant of

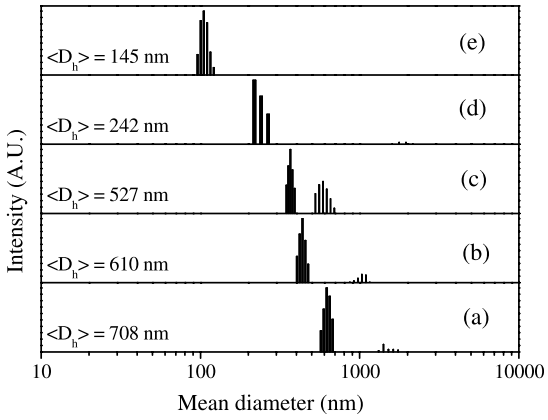

Fig. 3. The distribution of hydrodynamic diameter of samples at different polymerization time. (a) $t = 0$; (b) $t = 30$ min; (c) $t = 50$ min; (d) $t = 120$ min; (e) after shell cross-linking of nanospheres in (d).

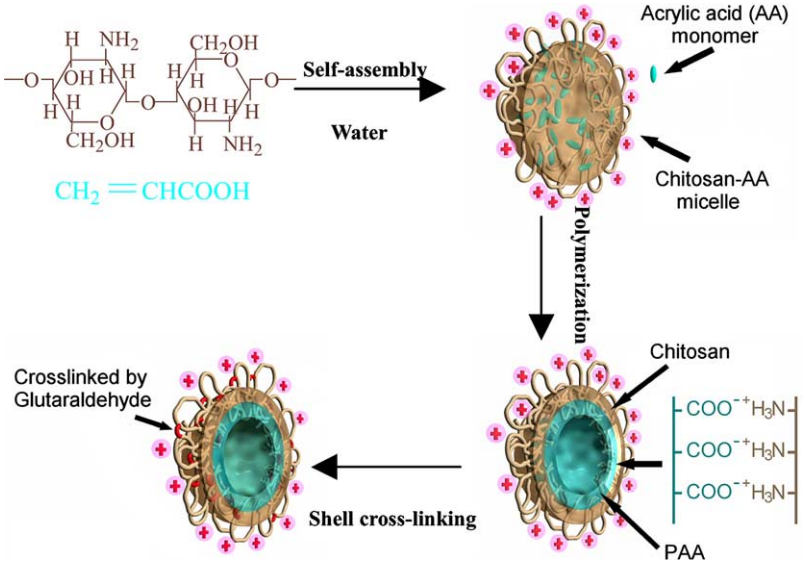

Fig. 4. Schematic illustration of formation process of CS–PAA hollow nanospheres.

these two opposing forces is the formation of the cavitation in nanospheres center with CS–PAA interpolyelectrolyte complexes as the inner shell and protonated CS chains as the outer shell. Progressively, the cross-linking reaction makes the CS outer shell fixed and also increases the packing density of CS in the shell of nanospheres.

Although there is a technological difficulty in microtomy of the non-cross-linked CS–PAA nanosphere samples to identify the role of cross-linking in the formation of hollow structure of the CS–PAA nanospheres since the nanospheres are not as hard as the cross-linked CS–PAA nanospheres, it is easy to understand that the hollow structure was formed in the polymerization process based on the cut-section TEM image of cross-linked CS–PAA nanospheres (Fig. 1(f)). First, the cross-linking reaction makes the spheres shrink progressively toward inside and not expand toward outside of spheres. Second, the cross-linking agent (i.e. glutaraldehyde) not only reacts with chitosan in the shell of spheres, but also reacts with chitosan molecules which lie inside of spheres. Thus, if the nanospheres are solid structure before the cross-linking (i.e. some chitosan in the core region of the sphere), we can not observe a hollow structure in the nanospheres after cross-linking reaction. Third, close examination of the sphere shells of Fig. 1(f), one can see that the dark ring (i.e. interpolyelectrolyte complex layer between CS and PAA) is present in the inner shell of these hollow nanospheres, indicating that the formation of hollow structure is induced by the polymerization of AA monomers inside core-shell assemblies.

3.3. Controlling the size of CS–PAA nanospheres

In the micelles and vesicles consisting of block copolymers, the control of micelle and vesicle size is strongly dependent on the block length of copolymer. However, in our cases, the size control of hollow nanospheres can be achieved by only changing the concentration of CS–AA assemblies in the reaction system before the polymerization. As seen in Table 1, with increasing initial CS–AA concentration over the range of 7.2–36 g/L, the intensity-average hydrodynamic diameter (D_h) of non-chemical cross-linking spheres obtained at the end of polymerization decreases from 500 to less than 100 nm. When the initial CS–AA concentration is around 43 g/L, the size of hollow sphere reaches 77 nm. Progressively increasing polymerization concentration to 50 g/L, the sphere size is not changed much. On the other hand, when the initial CS–AA concentration is below 7.2 g/L, no well-defined spheres can be obtained. As we have reported in early paper, before polymerization, CS and AA formed micelles [18]. These CS–AA micelles have positive zeta potential in the initial state. When the initial CS–AA concentration increased, the concentration of CS–AA micelle increased. The repulse force among the micelles induced by the surface charges of the micelles became stronger, which results in a compression for the CS–AA micelles and a reduction of the micelle size. Because the polymerization experiment mainly takes place in the micelles, the decreased micelle size leads to the decreasing of the average hydrodynamic diameter of formed nanospheres. This result indicates that the size of non-chemical cross-linked CS–PAA hollow spheres can be tuned by changing the polymerization concentration of CS–AA assemblies in the reaction system.

Table 1
Sphere size at different polymerization concentration

Concentration of CS and AA in reaction system[a] (g/L)	Hydrodynamic diameter[b] (nm)
7.2	495±7
14.4	242±9
29	239±11
36	93±3
43	77±2
50	78±6

[a] [Glucosamine unit in CS]:[acid in AA] =1.1:1.
[b] The size of noncross-linked spheres determined by DLS.

3.4. Cross-linking effect on the CS–PAA nanospheres

In present study we used glutaraldehyde (GA), an effective cross-linker for CS [22], to chemically cross-link CS–PAA hollow nanospheres. These cross-linked nanospheres can maintain stable in aqueous solution for more than 6 months at room temperature. Furthermore, these nanospheres can be separated by centrifugation at 8000 rpm from the aqueous solution and re-dispersed in water or buffers without aggregation. Compared with traditional nanometer polymeric particles such as polymeric micelles, and nanoparticles, the separation and the re-dispersing processes in our case are simple, and no cryoprotective agents and ultrasonication are required during freezing and re-dispersing process.

Since the chemical cross-linking procedure plays an important role in the control of sphere size and in the improvement of stability and mechanical properties of hollow nanospheres, it is necessary to study the effect of cross-linking time and the amount of GA added on CS–PAA hollow nanospheres. Fig. 5 displays the hydrodynamic diameter (D_h) of CS–PAA nanospheres measured by DLS as a function of the cross-linking time during the cross-linking. Two kinds of variation in the sphere size are observed depending on the cross-linking time. During the first 120 min, the size of CS–PAA nanospheres decreases from initial 242 to 145 nm. Then, the sphere size increases gradually to 185 nm at the cross-linking time of 400 min. Most likely, during the first 120 min, the cross-linking reaction takes place in the intra-spheres, especially in the outer shells of spheres, which leads to the shrinkage of spheres due to the consumption of amine groups and the increase in hydrophobicity. When the cross-linking time is beyond 120 min, the cross-linking reaction may take place not only in the intra-spheres but also inter-spheres, resulting in the increase in sphere size. DLS measurement shows that in contrast to unimodal distribution in sphere size at 120 min, the distribution in size is bimodal at cross-linking time of 400 min (data not shown). To investigate the influence of GA amount on the spheres size, the different GA amount was added into the reaction system by changing the molar ratio of GA to the amino groups on CS. As demonstrated in Table 2, the cross-linking reaction can cause the decrease in the size of spheres, and the size of spheres can be changed in range of 242 to 145 nm depending on the added amount of GA. However, when the ratio exceeds 1, macroscopical aggregation occurs and no nanospheres can be obtained.

Table 2
Effect of GA amount on sphere size

[CHO]:[NH_2][a]	Hydrodynamic diameter, (nm)	Zeta potential, (mV)
0	242±9	25.3±5.2
0.25:1	185.2±8.9	23.3±0.4
0.5:1	145.0±15	22.0±1.3
>1	No nanoparticles formed	

[a] Presents the ratio of aldehyde groups from GA to the amino groups from CS.

3.5. Response to the pH stimulation

As we have described above, these hollow nanospheres were formed by the electrostatic interaction between positively charged CS and negatively charged PAA. It is expected that changing pH values of medium may result in the variation in the size of the CS–PAA hollow nanospheres. Fig. 6 shows the size and ζ potential of the chemical cross-linked CS–PAA nanospheres measured by DLS and electrophoretic light scattering, respectively, after the nanospheres were immersed in different pH buffers for 24 h. Indeed, the hydrodynamic diameter of sphere is found to vary with pH, and the trend of change in sphere size shows a parabola shape with pH variation. The size of spheres reaches the minimum at pH in the range of 4.0 to 6.0, and becomes significantly large either in pH of 1 and 2 or in pH of 7.4. Meanwhile, the ζ potential shows a monotonous decrease and maintains a positive value in the pH range of 1.0 to 6.0. However, when the pH reaches 7.4, a negative ζ potential is observed. The negative zeta potentials at a pH above 7.0 is mostly caused by the adsorption of anions, such as the OH^- [23]. Further increasing pH to 8, the precipitation of the nanospheres occurs due to the complete deprotonation of CS.

Although a quantitative account is difficult to the behaviors of CS–PAA nanospheres in different pH medium because CS and PAA are the weak polyelectrolytes and their pK_a values changes in the presence of interpolyelectrolyte complexes, a qualitative explanation can be made. Key determinants in pH-induced changes of sphere size are the ionization degrees of CS and PAA in different pH medium and the electrostatic

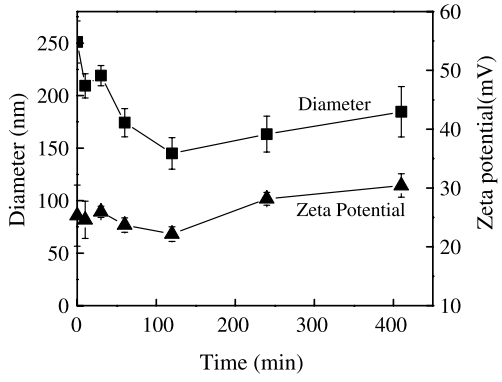

Fig. 5. Size and zeta potential variations of CS–PAA hollow nanospheres in the chemically cross-linking procedure.

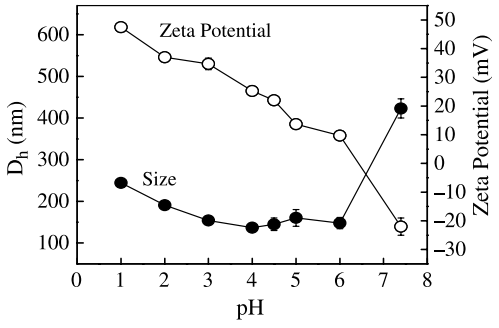

Fig. 6. The size and zeta potential of chemically cross-linked CS–PAA hollow nanoparticles after being immersed in different pH buffer.

repulsion between the same charged species. At low pH environment such as at pH 1 and 2, the CS is fully ionized but PAA is ionized minimally, which means that the interaction between the $-COO^-$ and $-NH_3^+$ is weakened. However, due to the shell-cross-linking and the stabilization of positively charged CS chains in the outer shells, the nanospheres structure is not destroyed. Thus, the CS–PAA nanosphere becomes swelling due to electrostatic repulsion between NH_3^+ groups in the outer shell, and an increase in size is observed. At pH 7.4, the situation is quite different, as the PAA in the inner shell is highly ionized while CS is ionized minimally. Thus, the electrostatic repulsion between COO^- groups of PAA becomes dominant inside nanospheres, which causes a swelling of whole structure. On the other hand, with the increasing of pH value, more and more anions, such as OH^- were adsorbed onto the surface of the nanospheres, resulting in a decrease of zeta potentials [23]. When the zeta potential closed to zero, the repulsion between nanospheres was weaken, leading to an aggregation of some nanospheres. Consequently, the dramatic increase in hydrated diameter was observed, which can be attributed to the swelling and aggregating of the CS–PAA nanospheres. When the pH of medium is in range of 4.0–6.0, both CS and PAA are partly ionized, and they can form compact interpolyelectrolyte complexes by electrostatic interaction. Therefore, a minimum in sphere size is reached.

3.6. Salt concentration and thermal effect on the size of CS–PAA nanospheres

Fig. 7 shows that the D_h value of nanospheres as a function of NaCl concentration at pH = 4.0. It can be seen that the size of CS–PAA hollow nanospheres changes with salt concentration. Unlike the situation for charged assemblies in which the addition of salt will decrease the size of assemblies due to the screening of charge at the surface of assemblies [24], in our case, over the salt concentration range from 0.1 to 2.0 M, the size of nanospheres increases from 140 to 170 nm. This increase in the spheres size reflects that the addition of salt not only screens the electrostatic charges at the surface of nanospheres but also screens the interaction between CS and

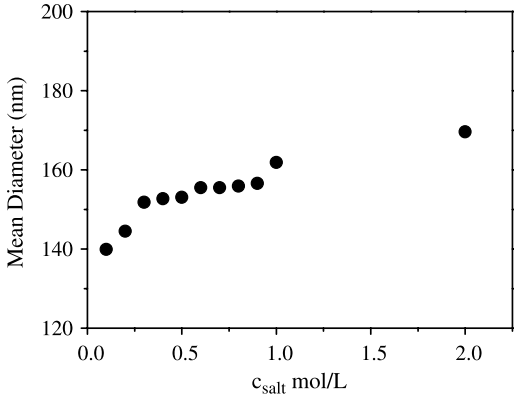

Fig. 7. Size dependence of chemically cross-linked CS–PAA hollow nanospheres on the added salt concentration.

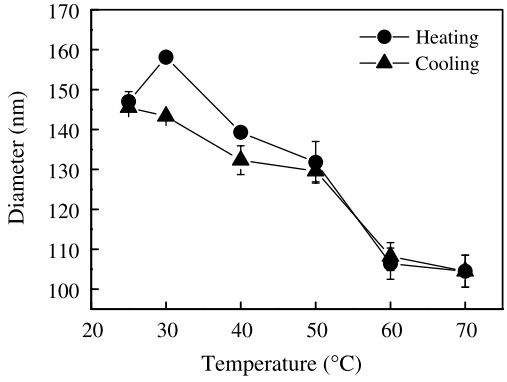

Fig. 8. Thermal behavior of chemically cross-linked CS–PAA hollow nanospheres in aqueous solution.

PAA in the nanospheres, which lead to an increase in the size of nanospheres.

The thermal sensitivity of CS–PAA nanospheres is investigated by monitoring the sphere size in aqueous solution (pH = 4.5) as a function of temperature. We found that the spheres size was dependent on the temperature (Fig. 8). The size of CS–PAA nanospheres increases when the temperature increases at the initial stage and then decreases with the progressive increase of temperature. When temperature drops, the nanospheres can return to their original size. The size change is reversible and reproducible with the heating and cooling.

A possible reason is that increasing temperature will increase the ionization degree of PAA and CS, which means that more PECs are formed and the electrostatic interaction between positively charged CS and negatively charged PAA increases. As a result, a decrease in sphere size is observed.

4. Conclusion

In this paper, we have demonstrated that CS–PAA hollow nanospheres can be synthesized by a core-template-free strategy in complete aqueous solution. The basis of this approach is that the amine groups on CS can interact with the carboxylic acid groups of acrylic acids to form core-shell assemblies. The cavity in the sphere center is spontaneously formed with the polymerization of AA monomers in CS–AA assemblies. The size of the hollow spheres can be adjusted by controlling the polymerization concentration and shell-cross-linking reaction, and the stability is much improved after the shell is cross-linked.

The synthesized nanospheres are stimuli-responsive. The size of the hollow nanospheres can be manipulated by changing the pH value, salt concentration and temperature. Furthermore, with heating and cooling the variation in size of hollow nanospheres is completely reversible and reproducible. Importantly, the surface of the hollow nanospheres is chemically active, as demonstrated by the shell cross-linking reaction, and provides the functional sites with chemical groups for subsequent chemical reactions at the surface (e.g. binding of biomolecules and surface grafting). Such hollow

nanospheres might be suitable to control drug release and gene delivery.

Acknowledgements

This work is supported by the Natural Science Foundation of China (No.20374026, No.10334020) and the 973 Program of MOST (No.2003CB615600).

References

[1] Prabhakaran K, Meneau F, Sankar G, Sumitomo K, Murashita T, Homma Y, et al. Adv Mater 2003;15:1522–6.
[2] Kim W, Choi HC, Shim M, Li YM, Wang DW, Dai HJ. Nano Lett 2002;2: 703–8.
[3] Haag R. Angew Chem Int Ed 2004;43:278–82.
[4] Martin CR, Kohli P. Nat Rev Drug Discov 2003;2:29–37.
[5] Panyam J, Labhasetwar V. Adv Drug Deliv Rev 2003;55:329–47.
[6] Cournarie F, Cheron M, Besnard M, Vauthier C. Eur J Pharm Biopharm 2004;57:171–9.
[7] Kakizawa Y, Kataoka K. Adv Drug Deliv Rev 2002;54:203–22.
[8] Gao Z, Lukyanov AN, Singhal A, Torchilin VP. Nano Lett 2002;2: 979–82.
[9] Langer R, Tirrell DA. Nature 2004;428:487–92.
[10] Stewart S, Liu GJ. Chem Mater 1999;11:1048–54.
[11] Huang H, Remsen EE, Kowalewski T, Wooley KL. J Am Chem Soc 1999;121:3805–6.
[12] General S, Rudloff J, Thunemann AF. Chem Commun 2002;534–5.
[13] Gittins DI, Caruso F. Adv Mater 2000;12:1947–8.
[14] Jang J, Ha H. Langmuir 2002;18:5613–8.
[15] Tiarks F, Landfester K, Antonietti M. Langmuir 2001;17:908–18.
[16] Sauer M, Streich D, Meier W. Adv Mater 2001;13:1649–51.
[17] Checot F, Lecommandoux S, Gnanou Y, Klok HA. Angew Chem Int Ed 2002;41:1340–3.
[18] Hu Y, Jiang XQ, Ding Y, Chen Q, Yang CZ. Adv Mater 2004;16:933–7.
[19] Ding Y, Hu Y, Jiang XQ, Zhang L, Yang CZ. Angew Chem Int Ed 2004; 46:6369–72.
[20] Qurashi MT, Blair HS, Allen SJ. J Appl Polym Sci 1992;46:255–61.
[21] McKenna BJ, Birkedal H, Bartl MH, Deming TJ, Stucky GD. Angew Chem Int Ed 2004;43:5652–5.
[22] Monteiro OAC, Airoldi C. Int J Biol Macromol 1999;26:119–28.
[23] Liu FT, Eisenberg A. J Am Chem Soc 2003;125:15059–64.
[24] Zhang Y, Jiang M, Zhao J, Wang Z, Dou J, Chen D. Langmuir 2005;21: 1531.